EXPLORING THE IMPACT OF DIFFUSION AND CHEMOTAXIS IN SPATIAL PATTERNS IN A MALARIA EPIDEMIC PDE MODEL: A TURING ANALYSIS

by

Bongekile Knowledge Gule

Submitted in partial fulfilment of the requirements
for the degree of Master of Science

at

Dalhousie University
Halifax, Nova Scotia
December 2023

Dalhousie University is located in Mi'kma'ki, the
ancestral and unceded territory of the Mi'kmaq.
We are all Treaty people.

Contents

LIST OF TABLES

LIST OF FIGURES

Abstract

The Ross model has been pivotal in studying malaria transmission dynamics, yet its limitations in describing parasite dispersal and other crucial factors hinder comprehensive control strategies. In this thesis, we introduce a partial differential equations (PDE) modeling framework that extends the Ross model with enhanced features, addressing aspects like parasite dispersal and attractiveness to humans.

Our research investigates the influence of diffusion and chemotaxis within the PDE model on spatial patterns in malaria transmission. Employing Turing analysis, we explore the impact of chemotactic movement on the emergence of spatial structures. We hypothesize that for stable eigenvalues in well-mixed conditions, there is a pattern formation for an eigenvalue that has positive real part in the presence of diffusion and chemotaxis for several allowable frequencies in a given domain.

This interdisciplinary study integrates mathematical modeling, biological insights, and computational methods, offering a nuanced understanding of the interplay between chemotaxis and diffusion in malaria propagation. The findings contribute valuable insights for designing targeted interventions and advancing our comprehension of malaria dynamics.

Glossary

Chemotaxis Chemotaxis is the process through which cells or biological species navigate within their environment by detecting and moving towards higher concentrations of chemical attractants. vii

Epidemic Model Models are used to understand the way infectious diseases spread through populations in epidemiology. vii

Malaria A parasistic disease caused by the bite of an Anopheles mosquito. vii

Pattern-Formation Distinct pattern resulting from the positive real part of eigenvalues when there is diffusion and chemotaxis. vii

Reaction-diffusion Describe the behaviour of a large range of chemical systems where diffusion of material competes with the production of that material by some form of chemical reaction. . vii

Stability Refers to negative or stable eigenvalues in the absence of diffusion and chemotaxis. vii

Turing Birfucation The Turing bifurcation is the basic bifurcation generating spatial pattern, was introduced by Alan Turing in a 1952 which elucidates the natural emergence of patterns in nature, such as stripes and spirals, from an initially uniform state. vii

Acknowledgements

I am immensely grateful to my supervisor, Professor David Iron, whose unwavering support, guidance, and mentorship were instrumental in the completion of this research. His dedication and encouragement have been invaluable in helping me realize my lifelong aspiration of attaining a Master's degree in Mathematics.

Additionally, I extend my heartfelt appreciation to the esteemed lecturers within the Department of Science at the University of Eswatini. Their expertise, encouragement, and support played a pivotal role in empowering me to accomplish my academic ambitions. I

am indebted to their collective efforts and contributions which have significantly enriched my educational journey and the completion of this research work.

Chapter 1 Introduction

Malaria is a parasitic disease transmitted by the bite of Anopheles mosquitoes and caused by Plasmodium falciparum, P. vivax, P. ovale wallikeri, P. ovale curtisi, P.malariae and P. knowlesi. The most common and prevalent species is P. falciparum in the Sub-Saharan Africa. Globally, there were an estimated 247 million malaria cases in 2021 in 84 malaria endemic countries (including the territory of French Guiana), an increase from 245 million in 2020, with most of this increase coming from countries in the World Health Organization(WHO) African Region[23]. The WHO African Region, with an estimated 234 million cases in 2021, accounted for about 95% of global cases with these four countries, Nigeria (27%), the Democratic Republic of the Congo (12%), Uganda (5%) and Mozambique (4%), accounting for almost half of all cases globally.

The percentage of total malaria deaths in children aged under 5 years reduced from 87% in 2000 to 76% in 2015. Since then there has been no change. About 96% of malaria deaths globally were in 29 countries, four of which accounted for just over half of all malaria deaths globally in 2021: Nigeria (31%), the Democratic Republic of the Congo (13%), the Niger (4%) and the United Republic of Tanzania (4%). Malaria deaths in the WHO African Region decreased from 841,000 in 2000 to 541,000 in 2018, before increasing to 599,000 in 2020. Estimated deaths decreased again to 593,000 in 2021. Globally, an estimated 2 billion malaria cases and 11.7 million malaria deaths in the period 2000–2021. Most of the cases (82%) and deaths (95%) averted were in the WHO African Region, followed by the WHO South-East Asia Region (cases 10% and deaths 3%).

The absence of a cure for malaria has a detrimental impact on the well-being of families, creating a cycle of persistent illness, hardship, and financial difficulties. Today, nearly half of the world's population, most of whom live in sub-Saharan Africa, is at risk of developing malaria and faces economic challenges[26]. Acquired immunity greatly influences how malaria affects an individual and a community. After repeated attacks of malaria a person may develop partially protective immunity.

The Ross model [25], which was the initial malaria model, offers an explanation for the relationship between the prevalence of mosquito populations and the incidence of malaria in human populations.

The model is given by

$$\begin{aligned} \frac{dI_h}{dt} &= abmI_m(1 - I_h) - rI_h, \\ \frac{dI_m}{dt} &= acI_h(1 - I_m) - \mu_2 I_m, \end{aligned} \tag{1}$$

where I_h, I_m are the infected human and mosquito population, a is the human biting rate, b is the proportion of bites that produce infection in human, c is the proportion of bites by which one susceptible mosquito becomes infected, m is the ratio of number of female mosquitoes to that of humans, r is the average recovery rate of humans and μ_2 is the per capita rate of mosquito mortality.

In this simple model, the total population of both humans and mosquitoes, N_h, N_m is assumed to be unchanging so that I_h, I_m are the proportion infected in each population. The first equation delineates alterations in the ratio of human infections, with new infections occurring based on factors such as the frequency of mosquito bites per person, the probabilities of a biting mosquito being infected (I_m), the bitten human being not infected ($1 - I_h$), and likelihood of an uninfected person becoming infected (b). Infections diminish as infected individuals return to the uninfected category at a characteristic recovery rate (rI_h). Likewise, the second equation outlines changes for the proportion of infected mosquitoes. The increase is contingent on factors like the number of mosquito bites per unit time (a), the probabilities of the biting mosquito being uninfected ($1 - I_m$), and the bitten human being infected (I_h). The decrease stems from the death of infected mosquitoes (I_m).

Ross, through his model, showed that reduction of mosquito numbers below a certain figure (Transmission threshold, R_0) was sufficient to counter malaria [25][18]. Several models have been developed by researchers who extended Ross's model by considering different factors, such as latent period of infection [18], acquired immunity[2][6], spatial and genetic heterogeneity of host and mosquito populations[12][10][9][24][30] .

Most infectious disease models assume homogeneous mixing among populations where individuals have the same contact rate [1][8]. Previous research suggests that heterogeneity alters disease establishment conditions compared to homogeneous mixing [27][26][22]. Research in the past[24] found that contact rates between subpopulations depend on individual mobility patterns, with higher mobility, leading to higher contact rates. In addition, when visit time decreases with distance, the establishment of the disease is more difficult

when the spatial arrangement is considered [24]. In this research, we investigate models wherein the spatial arrangement of hosts is divided into susceptible humans, susceptible mosquitoes, infected humans, and infected mosquitoes. We assume that the overall number of individuals (both humans and mosquitoes) is evenly distributed, and spatial distance had no effect on the spread of malaria. Our focus is primarily on infected mosquito movement to infected humans for feeding; we hypothesize that this preference contributes to pattern formation over time.

The Turing bifurcation is the basic bifurcation for generating spatial patterns. It was introduced by Alan Turing in a 1952 paper [32] which elucidates the natural emergence of patterns in nature, such as stripes and spirals, from an initially uniform state. The core concept of the Turing mechanism lies in the notion that a homogeneous equilibrium can be stable to homogeneous perturbations, but unstable to certain spatially varying perturbations, leading to a spatially varying steady state, that is, a spatially heterogeneous pattern. In the study of Turing bifurcation, different coefficients are examined to understand their role in pattern formation. They determine the stability and dynamics of the system, and different values can result in different pattern formations. Turing's theory has since been adapted by many mathematical researchers who have shown that a wide variety of patterns can be generated in computer simulations by varying diffusion coefficients, decay rates and other parameters in reaction-diffusion models [20][21][3].

In the process of diffusion, particles exhibit a net motion from areas of higher concentrations to those of lower concentrations. This concentration disparity establishes a gradient that prompts the particles to move, seeking to balance the differential concentrations. This phenomenon is closely linked to chemotaxis, a phenomenon describing the coordinated movement of cells or biological species directed from regions with lower chemoattractant concentration to those with a higher concentration of chemoattractant. In the context of anopheles mosquitoes, which exhibit a preference for feeding on infected humans, as reported by Warren [4] this results in a chemotactic response. Consequently, the mosquitoes actively move to locate humans for feeding, contributing to chemotaxis and giving rise to pattern formation as consequences of mosquito mobility.

In this study, we assume that the population of both mosquitoes (N_m) and humans (N_h) is constant, with susceptible mosquitoes and humans exhibiting logistic growth.

This is because the population growth of both humans and mosquitoes cannot continue to grow exponentially indefinitely, and the growth rate of both human and mosquito populations depends on the population size, which initially increases and eventually slows down and levels off when it reaches the maximum sustainable population size [31], which is called the carrying capacity. This leads to a more sustainable and self-regulating growth pattern for both mosquitoes and humans. Previous studies used to describe the population dynamics of mosquitoes and humans in the context of malaria transmission [17] showed that mosquito and human populations are assumed to have logistic growth.

In this study, we aim to investigate malaria transmission by utilizing a Turing analysis to analyze the pattern formation caused by the movement of infected mosquitoes as they feed on humans. The mathematical model used in this study is designed to incorporate an epidemic malaria model with diffusion, chemotaxis, and variability in population, specifically following the logistic growth law for both human and anopheles mosquito populations, and the death rates of both mosquito and human populations in a given domain. We want to show that there is a pattern formation for an eigenvalue that has a positive real part in the presence of diffusion and chemotaxis at several allowable frequencies in a given domain.

The remainder of this thesis is organized as follows. In the next section, we provide literature reviews for malaria, turing birfucation, and chemotaxis. In Section 2 a mathematical model of malaria with diffusion and chemotaxis is formulated. In Section 3, we provide results and analysis of our model, and the numerical simulations are also given. In Section 4, we provide a brief discussion. The final section concludes this thesis.

Chapter 2 Background

In this section, we review the background of malaria, the model formulation for Chemotaxis and reaction-diffusion of a system of two general equation using Turing analysis.

1 Malaria

Malaria spreads through the transfer of Plasmodium parasites between infected humans and susceptible mosquitoes, and vice versa. The duration of the life of a malaria-infected mosquito significantly influences transmission, with factors such as infection intensity, mosquito species, and environmental conditions playing a role[11]. In tropical locations, the average lifespan of Anopheles mosquitoes, including those carrying malaria, is 14–19 days [5], during which they can transmit the disease. On average, the parasite matures within the mosquito within approximately 10-14 days, making it infectious[15]. Only infected mosquitoes that survive beyond the incubation period of the malarial parasite will transmit the disease. Furthermore, millions of people die each year due to malaria, with more than half of them being children less than 5 years old. Infected humans generally recover faster than they succumb, whereas infected mosquitoes exhibit a significantly higher mortality rate than uninfected mosquitoes.

The malaria parasite manipulates both the mosquito and human hosts. Plasmodium infection boosts food intake in mosquitoes, significantly altering host metabolism to aid parasite development and potentially facilitating malaria transmission [33]. A previous study [4] found that infection with Plasmodium parasites, which cause malaria, can influence animal smell and people's attractiveness to mosquitoes. This causes dispersal of the mosquito population, which influences the spatial distribution of malaria, consequently leading to pattern formation over time.

The recovery period from malaria post-treatment is subject to variations based on factors such as infection severity, treatment type, and the individual's overall health. Research on antimalarial drugs has revealed that early diagnosis and treatment typically leads to successful complete recovery in humans [29]. However, people who live in areas where malaria is common can experience repeated infections and never fully recover between episodes of illness; the same applies to diagnoses that are not made early enough. Owing to the short lifespan of mosquitoes, we assume that they do not recover from malaria.

2 Chemotaxis

Chemotaxis is the process through which cells and biological species navigate within their environment by detecting and moving towards higher concentrations of chemical attractants[7]. Plasmodium parasites, the causative agents of malaria, have been found to influence the smell of animals and their attractiveness to mosquitoes[4]. From microscopic bacteria to large mammals, many motile organisms rely on chemotaxis for survival, leading them towards suitable hosts or nutrient sources; for example, mosquitoes locate humans by a smell, and pathogenic bacteria are attracted to substances released by their hosts. Chemotaxis also plays a crucial role in various fields such as embryogenesis, immunology, cancer growth, and invasion [28]. In our study, we present a derivation of the chemotactic response that transfers the focus from the detailed behavior of a given cell or organism to its average behavior in the positive direction, that is, positive chemotaxis, an idea based on a previous study[16].

We consider an organism(or cell) taking steps of length $\Delta\alpha$ to the left or right. Let $f(c)$ denote the average frequency of steps in a given direction, where c is the chemoattractant which itself is a function of x. For an organism centered at x, the average frequency of steps in the right and left directions is given by $f[c(x + \frac{1}{2}\alpha\Delta)]$ and $f[c(x - \frac{1}{2}\alpha\Delta)]$. Let $b(x)$ be the density of the organism centered at x. We want to find $J(x)$ the net flux of the organism per unit time in the direction increasing $c(x)$. Integrating the number of organisms $b(s)ds$ between s and $s + ds$ by the frequency of steps to the right, integrating over $(x - \Delta, x)$ and then subtracting the corresponding term describing the motion to the left gives

$$J(x) = \int_{x-\Delta}^{x} f[c(s + \frac{1}{2}\alpha\Delta)]b(s)ds - \int_{x}^{x+\Delta} f[c(s - \frac{1}{2}\alpha\Delta)]b(s)ds. \tag{2}$$

We keep only the lowest order terms in Δ, so that (2) becomes

$$J(x) \approx \Delta^2\{-f[c(x)]b'(x) + (\alpha - 1)f'[c(x)]b(x)c'(x)\}. \tag{3}$$

The first term

$$\mu[c(x)] = f[c(x)]\Delta^2,$$

is the diffusion term which is the non-chemotactic random motion of the organism. It is always positive. The second term

$$\chi[c(x)] = (\alpha - 1)f'[c(x)]\Delta^2,$$

is the chemotactic response. It can either be positive or negative.
Therefore this can be reduced to

$$J = -\mu \frac{db}{dx} + \chi \frac{dc}{dx}, \tag{4}$$

For $\alpha > 1$ the net frequency of steps to the right is governed by the concentration to the right of x. For $\alpha < 1$, on the other hand, this frequency is governed by the concentration to the left of x. The dependence of cell/ organism density $b(x,t)$ on position and time is described by the differential equation

$$\frac{\partial b}{\partial t} = -\vec{\nabla} \cdot \vec{J} \tag{5}$$

where the vector flux $\vec{J}$, which is the Keller-Segel(KS) model would be given by

$$\vec{J} = -\mu \vec{\nabla} b + \chi b \vec{\nabla} c. \tag{6}$$

The review article by Horstmann [14] provides a detailed introduction into the mathematics of the KS model for chemotaxis. The minimal model for KS [13] is given by

$$\begin{aligned} u_t &= \nabla(D\nabla u - \chi u \nabla v), \\ v_t &= \nabla^2 v + u - v, \end{aligned} \tag{7}$$

where u denotes the organism(cell) density in a given domain $\Omega \subseteq \mathbb{R}^n$, v denotes the concentration of the chemical signal, D is the diffusion coefficient (sometimes the called motility) of an organism(cell), and χ is the chemotactic sensitivity. A key property of the above is the ability of $\chi u \nabla v$ to give rise to spatial pattern formation, that is, when the chemical signal acts as an auto-attractant. In this study, our main focus is on the chemotactic sensitivity of infected mosquitoes to infected humans and how it influences the pattern formation in malaria transmission.

3 Turing Birfucation

The purpose of our study is to investigate the influence of chemotaxis on pattern formation in the context of malaria, specifically by analyzing the implications of the Turing bifurcation. Our objective is to gain a deeper understanding of how the movement of Anopheles mosquitoes towards humans impacts the resulting pattern formation. The general diffusion form of a two compound reaction-diffusion-chemotaxis system is as follows

$$\begin{aligned} A_t &= F(A, I) + D_A \Delta A, \\ I_t &= G(A, I) + D_I \Delta I + C(I A_x)_x, \end{aligned} \tag{8}$$

with boundary conditions on $\partial\Omega$ given by

$$\partial_x A = \partial_x I = 0, \tag{9}$$

where I is the organism(or cell) density, A is the chemical concentration, $F(A, I)$ describes the organism growth , $G(A, I)$ describes the production of the chemical signal, C is chemotactic sensitivity, D_A describes the diffusivity of organisms, D_I describes the diffusivity of the chemical signal , Δ is the Laplacian operator in Ω in the one dimensional interval [0,1] domain in $\mathbb{R}^n$, $\partial\Omega$ a boundary of Ω.
We assume that there exists constants $\bar{A}$ and $\bar{I}$ such that

$$\begin{aligned} F(\bar{A}, \bar{I}) &= 0, \\ G(\bar{A}, \bar{I}) &= 0. \end{aligned} \tag{10}$$

where $\bar{A}$, $\bar{I}$ is a spatially homogeneous solution. We now consider the stability of the steady state $\bar{A}$ and $\bar{I}$ to pertubations of various frequencies. We set

$$\begin{aligned} A &= \bar{A} + a\cos(kx)e^{\lambda t}, \\ I &= \bar{I} + i\cos(kx)e^{\lambda t}, \end{aligned} \tag{11}$$

where $|a| \ll |\bar{A}|$, $|i| \ll |\bar{I}|$ and $k = j\pi/L$, $j = 1, ...$ to satisfy boundary conditions. Our goal is to find a relationship between k and λ. We substitute this form into the reaction equations and since a and i are small, we only take into account the first nonzero term in the expansion. This results in the following problem

$$\begin{aligned} \lambda a &= F_A a + F_I i - D_A k^2 a, \\ \lambda i &= G_A a + G_I i - D_I k^2 i - C a \bar{A} k^2, \end{aligned} \tag{12}$$

where $F_A = \frac{\partial F}{\partial A}(\bar{A}, \bar{I})$, $F_I = \frac{\partial F}{\partial I}(\bar{A}, \bar{I})$, $G_A = \frac{\partial G}{\partial A}(\bar{A}, \bar{I})$, $G_I = \frac{\partial G}{\partial I}(\bar{A}, \bar{I})$.
We rewrite the eigenvalue problem in matrix notation

$$\lambda \begin{pmatrix} a \\ i \end{pmatrix} = \begin{pmatrix} F_A - D_A k^2 & F_I \\ G_A - C\bar{I}k^2 & G_I - D_I k^2 \end{pmatrix} \begin{pmatrix} a \\ i \end{pmatrix}. \tag{13}$$

If we have the following 2×2 matrix

$$M = \begin{pmatrix} a & b \\ c & d \end{pmatrix}, \tag{14}$$

then if

$$\begin{aligned} Tr(M) &= a + d, \\ Det(M) &= ad - bc, \end{aligned} \tag{15}$$

the two eigenvalues of M are then given by

$$\lambda_{1,2} = \frac{Tr \pm \sqrt{Tr^2 - 4Det}}{2}. \tag{16}$$

3).1 Well Mixed Condition

For this condition, we will require that in the absence of chemotaxis and diffusion, the spatially homogeneous solution, $(\bar{A}, \bar{I})$ is stable. The eigenvalue problem for the well mixed problem is

$$\lambda \begin{pmatrix} a \\ i \end{pmatrix} = \begin{pmatrix} F_A & F_I \\ G_A & G_I \end{pmatrix} \begin{pmatrix} a \\ i \end{pmatrix}. \tag{17}$$

Thus we will require

$$\begin{aligned} F_A + G_I &< 0, \\ F_A G_I - F_I G_A &> 0. \end{aligned} \tag{18}$$

For the eigenvalues we substitute the trace and determinant into (16). For the well mixed condition, we require that the eigenvalues to be stable. This is because localized structures are believed to grow from perturbations off of the spatially homogeneous solution. If the homogeneous solution is unstable in a well mixed solution, it will not persist long enough to experience pertubations.

3).2 Eigenvalue Problem With Diffusion And No Chemotaxis

The matrix of the eigenvalue problem with diffusion is given by

$$\lambda \begin{pmatrix} a \\ i \end{pmatrix} = \begin{pmatrix} F_A - D_A k^2 & F_I \\ G_A & G_I - D_I k^2 \end{pmatrix} \begin{pmatrix} a \\ i \end{pmatrix}. \tag{19}$$

From (18) $F_A + G_I < 0$ hence the condition

$$F_A + G_I - k^2(D_A + D_I) < 0. \tag{20}$$

Thus the trace condition is satisfied. For the determinant we have

$$(F_A - D_A k^2)(G_I - D_I k^2) - F_I G_A. \tag{21}$$

Expanding out the above equation we get

$$D_A D_I k^4 - (D_I F_A + D_A G_I)k^2 + (F_A G_I - F_I G_A). \tag{22}$$

From (18) the third term is positive hence to have $Det > 0$ we require

$$D_I F_A + D_A G_I < 0.$$

For eigenvalues we substitute the trace(T) and determinant(D) into (16).
The condition for spike formation $D_I F_A + D_A G_I < 0$ can not be met when $D_I = D_A$ due to the well mixed requirement. This means that patterns are not possible when the two diffusivities are equal.

3).3 Eigenvalue Problem With Diffusion And Chemotaxis

The matrix for the eigenvalue problem with diffusion and chemotaxis is given by

$$\lambda \begin{pmatrix} a \\ i \end{pmatrix} = \begin{pmatrix} F_A - D_A k^2 & F_I \\ G_A - C\bar{I}k^2 & G_I - D_I k^2 \end{pmatrix} \begin{pmatrix} a \\ i \end{pmatrix}. \tag{23}$$

From (18) the Trace(T) is such that

$$T = F_A + G_I - k^2(D_A + D_I) < 0. \tag{24}$$

and the Determinant(D) is

$$(F_A - D_A k^2)(G_I - D_I k^2) - F_I(G_A - C\bar{I}k^2). \tag{25}$$

When the specified conditions are met, pattern formation becomes feasible, necessitating adherence to these steps in the case of a 2×2 system. For systems comprising more than 2 equations, the potential for pattern formation exists when stable eigenvalues are present under well-mixed conditions. Therefore, it is essential to exclusively assess eigenvalues for systems with more than 2 equations in such instances.
In a finite domain of length L, the allowable values of ω are $j\frac{\pi}{L}$ for some integer j. For larger domains the frequencies are closer together.This implies that the bigger the domain the more likely it is that we will have an allowable frequency which will grow.

Chapter 3 Mathematical Model

In our general model, we distinguish the human population into susceptible and infected classes, wherein we assume individuals transition from infected back to susceptible following treatment. Consequently, humans are represented by an SIS model. Conversely, mosquitoes, characterized by a brief lifespan post-infection, are modeled using a simplified SI model with only susceptible and infected classes resulting to SI model. To delve into the intricacies of the reaction-diffusion model, our initial focus is on exploring pattern formation incorporating chemotaxis and diffusion in a comprehensive 4×4 model. The general model is given by

$$\begin{aligned}
\frac{dI_h}{dt} &= D_{h1}\frac{\partial^2 I_h}{\partial x^2} + F(I_h, S_h, I_m, S_m),\\
\frac{dS_h}{dt} &= D_{h2}\frac{\partial^2 S_h}{\partial x^2} + G(I_h, S_h, I_m, S_m),\\
\frac{dI_m}{dt} &= D_m\frac{\partial^2 I_m}{\partial x^2} + H(I_h, S_h, I_m, S_m) + C_1\frac{d}{dx}(I_m\frac{dI_h}{dx}) + C_2\frac{d}{dx}(I_m\frac{dS_h}{dx}),\\
\frac{dS_m}{dt} &= D_m\frac{\partial^2 S_m}{\partial x^2} + P(I_h, S_h, I_m, S_m) + C_1\frac{d}{dx}(S_m\frac{dI_h}{dx}) + C_2\frac{d}{dx}(S_m\frac{dS_h}{dx}),
\end{aligned} \tag{26}$$

in the domain $(-L, L)$ with boundary conditions

$$\frac{\partial I_h}{\partial x} = \frac{\partial S_h}{\partial x} = \frac{\partial I_m}{\partial x} = \frac{\partial S_m}{\partial x} = 0, \tag{27}$$

where F, G are the infected and susceptible human interaction functions, H, P are the infected and susceptible mosquitoes interaction functions S_h, I_h, S_m, I_m represents susceptible humans, infected humans, susceptible mosquitoes, and infected mosquitoes. D_{h1} and D_{h2} are diffusion coefficients for infected and susceptible humans, C_1, C_2 are the chemotaxis coefficients, since mosquitoes are attracted to humans.
We assume that the exist constants $\bar{I_h}, \bar{S_h}, \bar{I_m}, \bar{S_m}$ such that

$$F(\bar{I_h}, \bar{S_h}, \bar{I_m}, \bar{S_m}) = G(\bar{I_h}, \bar{S_h}, \bar{I_m}, \bar{S_m}) = H(\bar{I_h}, \bar{S_h}, \bar{I_m}, \bar{S_m}) = P(\bar{I_h}, \bar{S_h}, \bar{I_m}, \bar{S_m}) = 0. \tag{28}$$

We now consider the stability of the steady state $\bar{I_h}, \bar{S_h}, \bar{I_m}, \bar{S_m}$ to perturbations of various frequencies.

We substitute

$$\begin{aligned} I_h &= \bar{I_h} + a\cos\{\omega x\}e^{\lambda t}, \\ S_h &= \bar{S_h} + b\cos\{\omega x\}e^{\lambda t}, \\ S_m &= \bar{S_m} + i\cos\{\omega x\}e^{\lambda t}, \\ I_m &= \bar{I_m} + d\cos\{\omega x\}e^{\lambda t}. \end{aligned} \tag{29}$$

where $|a| \ll \bar{I_h}$, $|i| \ll \bar{S_m}$, $|b| \ll \bar{S_h}$, $|d| \ll \bar{I_m}$ and $\omega = j\pi$ for $j = 1, ...$ to satisfy boundary conditions.
This leads to the following problem

$$\begin{aligned} \lambda a &= -D_{h1}a\omega^2 + F_{Ih}a + F_{Sh}b + F_{Im}d + F_{Sh}i, \\ \lambda b &= -D_{h2}b\omega^2 + G_{Ih}a + G_{Sh}b + G_{Im}d + G_{Sm}i, \\ \lambda d &= -D_m d\omega^2 + H_{Ih}a + H_{Sh}b + H_{Im}d + H_{Sm}i - C_1 a\omega^2\bar{I_m} - C_2 b\omega^2\bar{I_m}, \\ \lambda i &= -D_m i\omega^2 + P_{Ih}a + P_{Sh}b + P_{Im}d + P_{Sm}i - C_1 a\omega^2\bar{S_m} - C_2 b\omega^2\bar{S_m}, \end{aligned} \tag{30}$$

where we asssume the constants
$F_{Ih} = \frac{\partial F}{\partial I_h}(\bar{I_h}, \bar{S_h}, \bar{I_m}, \bar{S_m})$, $F_{Sh} = \frac{\partial F}{\partial S_h}(\bar{I_h}, \bar{S_h}, \bar{I_m}, \bar{S_m})$,
$F_{Im} = \frac{\partial F}{\partial I_m}(\bar{I_h}, \bar{S_h}, \bar{I_m}, \bar{S_m}, F_{Sm}) = \frac{\partial F}{\partial S_m}(\bar{I_h}, \bar{S_h}, \bar{I_m}, \bar{S_m})$,
$G_{Ih} = \frac{\partial G}{\partial I_h}(\bar{I_h}, \bar{S_h}, \bar{I_m}, \bar{S_m})$, $G_{Sh} = \frac{\partial G}{\partial S_h}(\bar{I_h}, \bar{S_h}, \bar{I_m}, \bar{S_m})$,
$G_{Im} = \frac{\partial G}{\partial I_m}(\bar{I_h}, \bar{S_h}, \bar{I_m}, \bar{S_m})$, $G_{Sm} = \frac{\partial G}{\partial S_m}(\bar{I_h}, \bar{S_h}, \bar{I_m}, \bar{S_m})$,
$H_{Ih} = \frac{\partial H}{\partial I_h}(\bar{I_h}, \bar{S_h}, \bar{I_m}, \bar{S_m})$, $H_{Sh} = \frac{\partial H}{\partial S_h}(\bar{I_h}, \bar{S_h}, \bar{I_m}, \bar{S_m})$,
$H_{Im} = \frac{\partial H}{\partial I_m}(\bar{I_h}, \bar{S_h}, \bar{I_m}, \bar{S_m})$, $H_{Sm} = \frac{\partial H}{\partial S_m}(\bar{I_h}, \bar{S_h}, \bar{I_m}, \bar{S_m})$,
$P_{Ih} = \frac{\partial P}{\partial I_h}(I_h, S_h, \bar{I_m}, S_m)$, $P_{Sh} = \frac{\partial P}{\partial S_h}(\bar{I_h}, \bar{S_h}, \bar{I_m}, \bar{S_m})$,
$P_{Im} = \frac{\partial P}{\partial I_m}(\bar{I_h}, \bar{S_h}, \bar{I_m}, \bar{S_m})$, $P_{Sm} = \frac{\partial P}{\partial S_m}(\bar{I_h}, \bar{S_h}, \bar{I_m}, \bar{S_m})$.
We rewrite the eigenvalue problem in matrix notation. This is similar to taking the Jacobian for each equation. Thus

$$\lambda \begin{pmatrix} a \\ b \\ d \\ i \end{pmatrix} = \begin{pmatrix} -D_{h1}\omega^2 + F_{Ih} & F_{Sh} & F_{Im} & F_{Sm} \\ G_{Ih} & G_{Sh} - D_{h2}\omega^2 & G_{Im} & G_{Sm} \\ -C_1\bar{I_m}\omega^2 + H_{Ih} & H_{Sh} - C_2\omega^2\bar{I_m} & H_{Im} - D_m\omega^2 & H_{Sm} \\ P_{Ih} - C_1\bar{S_m}\omega^2 & P_{Sh} - C_2\bar{S_m}\omega^2 & P_{Im} & P_{Sm} - D_m\omega^2 \end{pmatrix} \begin{pmatrix} a \\ b \\ d \\ i \end{pmatrix}. \tag{31}$$

What we will do now is to find under what conditions will individual frequencies grow, Or what values of k may result in with positive real part.

3 a) Well-Mixed Condition

If we repeat the process, this time without any diffusion and chemotaxis, (26) reduces to

$$\lambda \begin{pmatrix} a \\ b \\ d \\ i \end{pmatrix} = \begin{pmatrix} F_{Ih} & F_{Sh} & F_{Im} & F_{Sm} \\ G_{Ih} & G_{Sh} & G_{Im} & G_{Sm} \\ H_{Ih} & H_{Sh} & H_{Im} & H_{Sm} \\ P_{Ih} & P_{Sh} & P_{Im} & P_{Sm} \end{pmatrix} \begin{pmatrix} a \\ b \\ d \\ i \end{pmatrix}. \tag{32}$$

It is required that the fixed point of the above non-spatial system be stable, and we must have all eigenvalues with negative real part at the fixed point. If the real part of the leading eigenvalue becomes positive when diffusion is turned on ($D_{h1}, D_{h2}, D_m > 0$), that is, if the fixed points become unstable in the diffusive system, then we speak of a Turing instability.

3 b) The Eigenvalue Problem With Diffusion And No Chemotaxis

The addition of diffusion leads to the following system

$$\lambda \begin{pmatrix} a \\ b \\ d \\ i \end{pmatrix} = \begin{pmatrix} -D_{h1}\omega^2 + F_{Ih} & F_{Sh} & F_{Im} & F_{Sm} \\ G_{Ih} & G_{Sh} - D_{h2}\omega^2 & G_{Im} & G_{Sm} \\ H_{Ih} & H_{Sh} & H_{Im} - D_m\omega^2 & H_{Sm} \\ P_{Ih} & P_{Sh} & P_{Im} & P_{Sm} - D_m\omega^2 \end{pmatrix} \begin{pmatrix} a \\ b \\ d \\ i \end{pmatrix}. \tag{33}$$

3 c) Eigenvalue Problem With Diffusion And Chemotaxis

The addition of both diffusion and chemotaxis leads to the folloowing

$$\lambda \begin{pmatrix} a \\ b \\ d \\ i \end{pmatrix} = \begin{pmatrix} -D_{h1}\omega^2 + F_{Ih} & F_{Sh} & F_{Im} & F_{Sm} \\ G_{Ih} & G_{Sh} - D_{h2}\omega^2 & G_{Im} & G_{Sm} \\ -C_1\bar{I_m}\omega^2 + H_{Ih} & H_{Sh} - C_2\omega^2\bar{I_m} & H_{Im} - D_m\omega^2 & H_{Sm} \\ P_{Ih} - C_1\bar{S_m}\omega^2 & P_{Sh} - C_2\bar{S_m}\omega^2 & P_{Im} & P_{Sm} - D_m\omega^2 \end{pmatrix} \begin{pmatrix} a \\ b \\ d \\ i \end{pmatrix}. \tag{34}$$

The fixed points become unstable resulting to Turing instability with eigenvalues having positive real part leading to pattern formation.

4 Partial Differential Equation Model With Diffusion And Chemotaxis

We investigate the effects of spatial variations in the diffusion and chemotaxis coefficients of four interacting individuals, with concentrations $I_h(x,t)$, $S_h(x,t)$, $I_m(x,t)$, $S_m(x,t)$. We consider, in particular, spatially heterogeneous steady state solutions of the non-dimensionalised reaction-diffusion-chemotaxis system in the domain $(-L, L)$. The model below illustrates the relationship between the four components

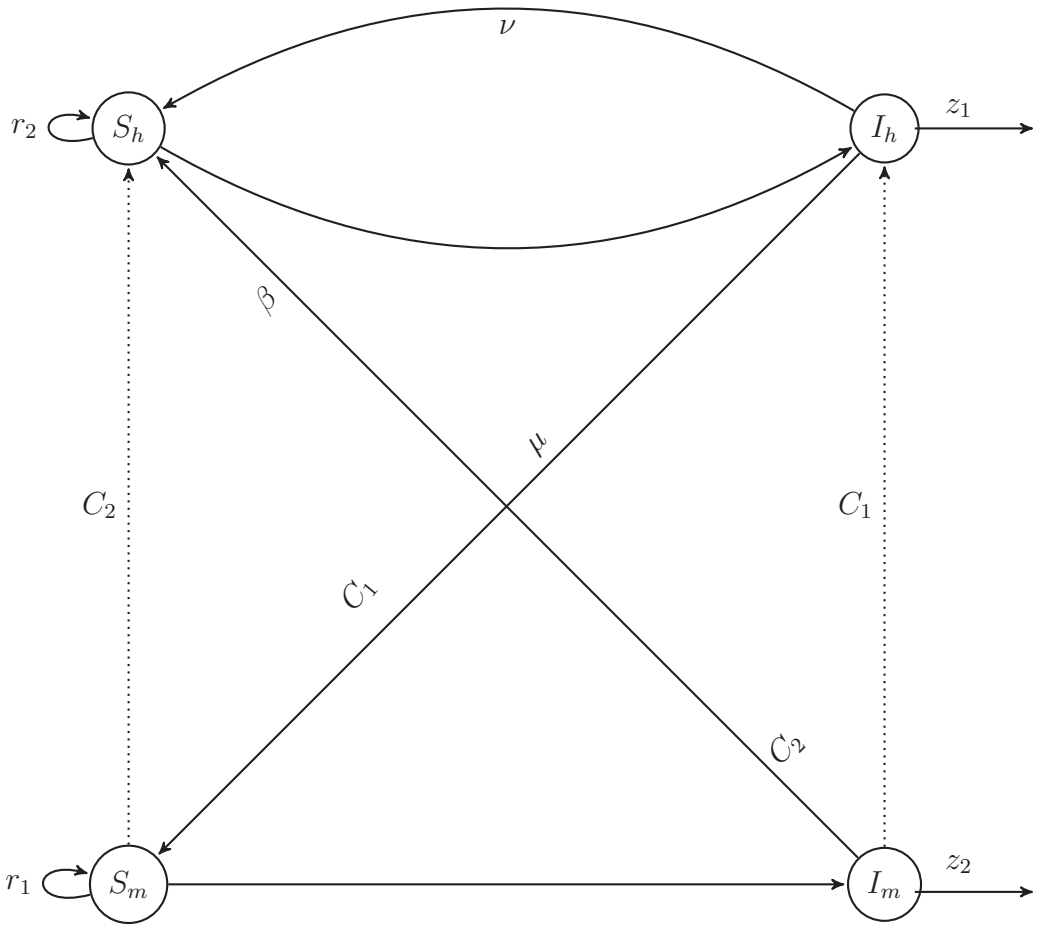

Figure 1: Malaria model with diffusion and chemotaxis. The various parameters are described below.

The graph above leads to the equations below

$$\begin{aligned}
\frac{d}{dt}(I_h) &= D_{h1}\frac{\partial^2}{\partial x^2}(I_h) + \beta S_h I_m - \nu I_h - z_1 I_h, \\
\frac{d}{dt}(S_h) &= D_{h2}\frac{\partial^2}{\partial x^2}(S_h) - \beta S_h I_m + \nu I_h + r_2 S_h(N_h - S_h), \\
\frac{d}{dt}(I_m) &= D_m\frac{\partial^2}{\partial x^2}(I_m) + \mu I_h S_m - z_2 I_m + C_1\frac{d}{dx}(I_m\frac{d}{dx}(I_h)) + C_2\frac{d}{dx}(I_m\frac{d}{dx}(S_h)), \\
\frac{d}{dt}(S_m) &= D_m\frac{\partial^2}{\partial x^2}(S_m) + r_1(S_m + I_m)(N_m - S_m - I_m) - \mu I_h S_m + C_1\frac{d}{dx}(S_m\frac{d}{dx}(I_h)) \\
&\quad + C_2\frac{d}{dx}(S_m\frac{d}{dx}(S_h)),
\end{aligned} \tag{35}$$

in the domain $(-L, L)$ with boundary conditions

$$\frac{\partial I_h}{\partial x} = \frac{\partial S_h}{\partial x} = \frac{\partial I_m}{\partial x} = \frac{\partial S_m}{\partial x} = 0, \tag{36}$$

where S_h, I_h, S_m, I_m represents the number of susceptible humans, infected humans, susceptible mosquitoes, and infected mosquitoes, D_{h1} and D_{h2} are diffusion coefficients for infected and susceptible humans, β is the infectious mosquito to susceptible human transmission rate in humans, ν is the infected human partial recovery rate, z_1 is the death rate for infected humans due to malaria, z_2 is the death rate for infected mosquitoes due to malaria, r_2 human growth rate, D_m the mosquito diffusivity, μ is the infectious human to susceptible mosquito transmission rate in mosquitoes, r_1 the mosquito growth rate and C_1, C_2 are chemotaxis coefficients.

The first equation shows the fraction of humans infected with malaria. A susceptible human (S_h) becomes infected through a mosquito bite from an infected mosquito (I_m), with a transmission rate denoted by β. This transmission can lead to the death of some infected individuals, represented by $z_1 I_h$ due to malaria. Additionally, we assume that individuals partially recover after getting treatment and thus transition from infected νI_h individuals to susceptible humansS_h. The spread of infected humansI_h is governed by the first term, characterized by a diffusion coefficient denoted as D_{h1}.

The second equation illustrates the proportion of susceptible humans. When a susceptible individual (S_h) is bitten by an infected mosquito with a transmission rate β, it becomes infected and transitions from the susceptible class to infected humans. We assume that individuals partially recover leave the infected category (νI_h) to become susceptible humans. The third term, $r_2 S_h(N_h - S_h)$, denotes the logistic growth of susceptible humans. Here, we

assume human population size (N_h) is the carrying capacity. The growth rate is denoted by r_2, and $(N_h - S_h)$ indicates the additional individuals that can be accommodated in the susceptible population before reaching the carrying capacity (N_h). The spread of infected humans is governed by the first term, characterized by a diffusion coefficient denoted as D_{h2}.

The third term represents the fraction of mosquitoes infected with malaria. Malaria transmission occurs when a susceptible mosquito (S_m) bites an infected human (I_h) at a rate denoted by μ, resulting in the death of infected mosquitoes (I_m) due to their limited lifespan, with a death rate specified by z_2. As mosquitoes actively seek blood meals, Plasmodium parasite infection, causing malaria, can influence how animals smell and human attractiveness to mosquitoes. This phenomenon leads to chemotaxis interactions among infected mosquitoes, infected humans, and susceptible humans, characterized by chemotactic coefficients C_1 and C_2, where $C_1 > C_2$ reflecting the mosquito preference for infected humans. The spread of infected mosquitoes is governed by the first term, characterized by a diffusion coefficient denoted as D_m.

The fourth equation illustrates the proportion of susceptible mosquitoes. When a susceptible mosquito (S_m) bites an infected human, malaria is transmitted at a rate denoted by β, causing the susceptible mosquito to transition to the infected mosquito class. We assume a constant mosquito population size (N_m). The growth rate is designated as r_2, and $(N_m - S_m - I_m)$ indicates the additional individuals that can be accommodated in the susceptible population before reaching the carrying capacity (N_m). In this scenario, susceptible mosquitoes are born from other susceptible mosquitoes, and we also posit that infected mosquitoes give birth to susceptible mosquitoes. As mentioned earlier, mosquitoes exhibit a preference for infected humans, influencing the interaction between susceptible mosquitoes and infected humans with a chemotactic coefficient C_1. Additionally, the interaction between susceptible humans and mosquitoes involves a chemotactic coefficient C_2, where, once again, $C_1 > C_2$. The spread of infected mosquitoes is governed by the first term, characterized by a diffusion coefficient denoted as D_m.

We consider the stability of the steady state $\bar{I_h}, \bar{S_h}, \bar{S_m}, \bar{I_m}$ to perturbations of various frequencies

$$I_h = \bar{I_h} + a\cos(kx)e^{\lambda t}, \tag{37}$$

$$I_m = \bar{I_m} + b\cos(kx)e^{\lambda t}, \tag{38}$$

$$S_h = \bar{S_h} + d\cos(kx)e^{\lambda t}, \tag{39}$$

$$S_m = \bar{S_m} + i\cos(kx)e^{\lambda t}. \tag{40}$$

4 a) Well-Mixed Condition

The eigenvalue problem of our model (35) without diffusion and chemotaxis is given by

$$\lambda \begin{pmatrix} a \\ b \\ d \\ i \end{pmatrix} = \begin{pmatrix} -z_1-\nu & \beta I_m & \beta S_h & 0 \\ \nu & -\beta I_m + r_2(N_h - S_h) - r_2 S_h & -\beta S_h & 0 \\ \mu S_m & 0 & -z_2 & \mu I_h \\ -\mu S_m & 0 & 0 & r_1(N_h - S_m) - r_1 S_m - \mu I_h \end{pmatrix} \begin{pmatrix} a \\ b \\ d \\ i \end{pmatrix}. \tag{41}$$

4 b) Eigenvalue Problem With Diffusion And No Chemotaxis

The eigenvalue problem of our model (35) with diffusion is given by

$$\lambda \begin{pmatrix} a \\ b \\ d \\ i \end{pmatrix} = \begin{pmatrix} -z_1-\nu-D_{h1}\omega^2 & \beta I_m & \beta S_h & 0 \\ \nu & -\beta I_m + r_2(N_h - S_h) - r_2 S_h - D_{h2}\omega^2 & -\beta S_h & 0 \\ \mu S_m & 0 & -z_2 - D_m\omega^2 & \mu I_h \\ -\mu S_m & 0 & 0 & r_1(N_h - S_m) - r_1 S_m - \mu I_h - D_m\omega^2 \end{pmatrix} \begin{pmatrix} a \\ b \\ d \\ i \end{pmatrix}. \tag{42}$$

4 c) Eigenvalue Problem With Diffusion And Chemotaxis

The eigenvalue problem of our model (35) with diffusion and chemotaxis is given by

$$\lambda \begin{pmatrix} a \\ b \\ d \\ i \end{pmatrix} = \begin{pmatrix} -z_1 - \nu - D_{h1}\omega^2 & \beta I_m & \beta S_h & 0 \\ \nu & -\beta I_m + r_2(N_h - S_h) - r_2 S_h - D_{h2}\omega^2 & -\beta S_h & 0 \\ \mu S_m - C_1 I_m \omega^2 & -C_2 I_m \omega^2 & -z_2 - D_m \omega^2 & \mu I_h \\ -\mu S_m - C_1 S_m \omega^2 & -C_2 S_m \omega^2 & 0 & r_1(N_h - S_m) - r_1 S_m - \mu I_h - D_m \omega^2 \end{pmatrix} \begin{pmatrix} a \\ b \\ d \\ i \end{pmatrix}. \tag{43}$$

Chapter 4 Results And Analysis

We now consider specific set of parameter values and we will show that Turing birfurcation occurs and pattern formations are robust. The values used for numerical simulation for (35) are as follows

$$D_{h1} = 1, \tag{44}$$
$$D_{h2} = 1, \tag{45}$$
$$D_m = 0.25, \tag{46}$$
$$C_1 = 150, \tag{47}$$
$$C_2 = 15, \tag{48}$$
$$z_1 = 0.00002, \tag{49}$$
$$z_2 = 1, \tag{50}$$
$$\beta = 10, \tag{51}$$
$$\mu = 0.00025, \tag{52}$$
$$\nu = 0.002, \tag{53}$$
$$r_1 = 20, \tag{54}$$
$$r_2 = 2, \tag{55}$$
$$N_h = 100, \tag{56}$$
$$N_m = 13000, \tag{57}$$
$$L = 50. \tag{58}$$

By solving the linear terms in (35) using Maple, this results in spatially homogeneous equilibrium solutions which are as follows

Number	$\bar{I_h}$	$\bar{S_h}$	$\bar{I_m}$	$\bar{S_m}$
1	0	0	0	0
2	0	0	0	100
3	0	0	100	100
4	4802.421830	119.9884731	0.009605766368	99.93996973
5	7.996157540×10^6	96.01536656	19.98719453	0.04803075281

Table 1: Equilibrium Solutions for the malaria model (35)

Solution number 4 together with (44) was then used in Maple[19] to solve the eigenvalue problem as a function of ω in the domain $(-L, L)$. The results are given below.

5 Partial Differential Equation Model With Diffusion And Chemotaxis

5).1 Well-Mixed Condition

The real part of the eigenvalues of (41) are given by

$$\begin{aligned} Re[\lambda_1(\omega)] &= -0.000479933036173108, \\ Re[\lambda_2(\omega)] &= -0.999517231910559, \\ Re[\lambda_3(\omega)] &= -1998.79939400159, \\ Re[\lambda_4(\omega)] &= -999.925556933465. \end{aligned} \tag{59}$$

All the eigenvalues have negative real part thus the system is stable in well-mixed condition.

5).2 Eigenvalue Problem With Diffusion And No Chemotaxis

Graphical solutions were employed to depict the real part of the eigenvalues using Maple in (42). Each eigenvalue was graphed against the frequency, and the outcomes are presented in figure 6;

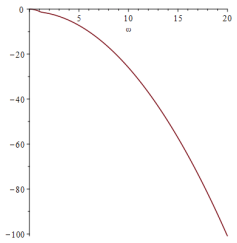

Figure 2:
Re(λ_1)vs(ω)

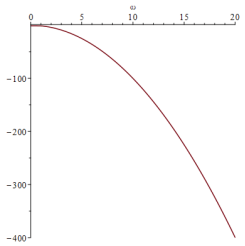

Figure 3:
Re(λ_2)vs(ω)

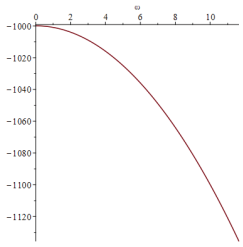

Figure 4:
Re(λ_3)vs(ω)

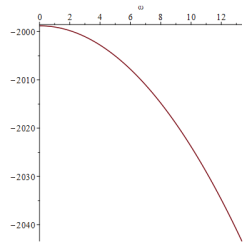

Figure 5:
Re(λ_4)vs(ω)

Figure 6: The graph of real eigenvalues vs frequency(ω) with diffusion and no chemotaxis in Maple

The above graphs show that all the real parts of each eigenvalue are negative at all times in the domain $(-L, L)$ hence, no pattern formation is possible.

5).3 Eigenvalue Problem With Diffusion And Chemotaxis

We proceeded to graph the real part of the eigenvalues (43), yielding the outcomes

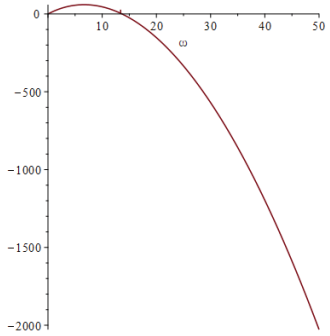

Figure 7: $\mathrm{Re}(\lambda_1)\mathrm{vs}(\omega)$

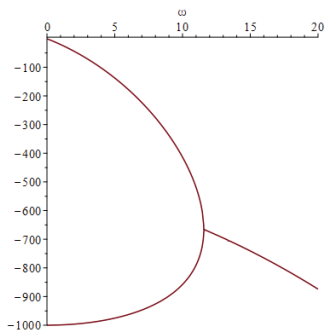

Figure 8: $\mathrm{Re}(\lambda_2, \lambda_3)\mathrm{vs}(\omega)$

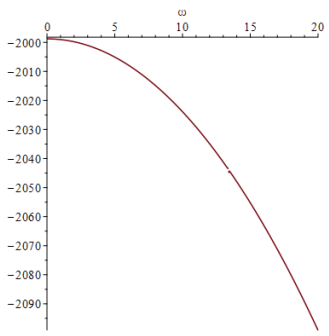

Figure 9: $\mathrm{Re}(\lambda_4)\mathrm{vs}(\omega)$

Figure 10: The graphs for real eigenvalues vs frequency (ω) with diffusion and chemotaxis plotted in Maple

In light of this, we have grouped them together based on their real part, with λ_1 corresponding to several allowable frequencies within the range of $0 < \omega < 14$ in the domain of $(-L, L)$ with positive real part. It is worth noting that eigenvalues 2, 3, and 4 possess negative values for all times.

The most direct way to prove the existence of Turing's principle is to apply perturbations to the spatial pattern of the model given by (35) and observe their dynamics, which leads to the initial conditions

$$S_h = 1000, \tag{60}$$

$$I_h = 1, \tag{61}$$

$$I_m = 100 + 0.2\cos\{0.2x\}, \tag{62}$$

$$S_m = 100 + 0.2\cos\{0.2x\}. \tag{63}$$

The graphs below depict the modeling of each population's initial conditions simulated using FlexPDE6. They illustrate the global maximum equilibrium that each population can attain, and these graphs remain in equilibrium for the entire duration after a certain period.

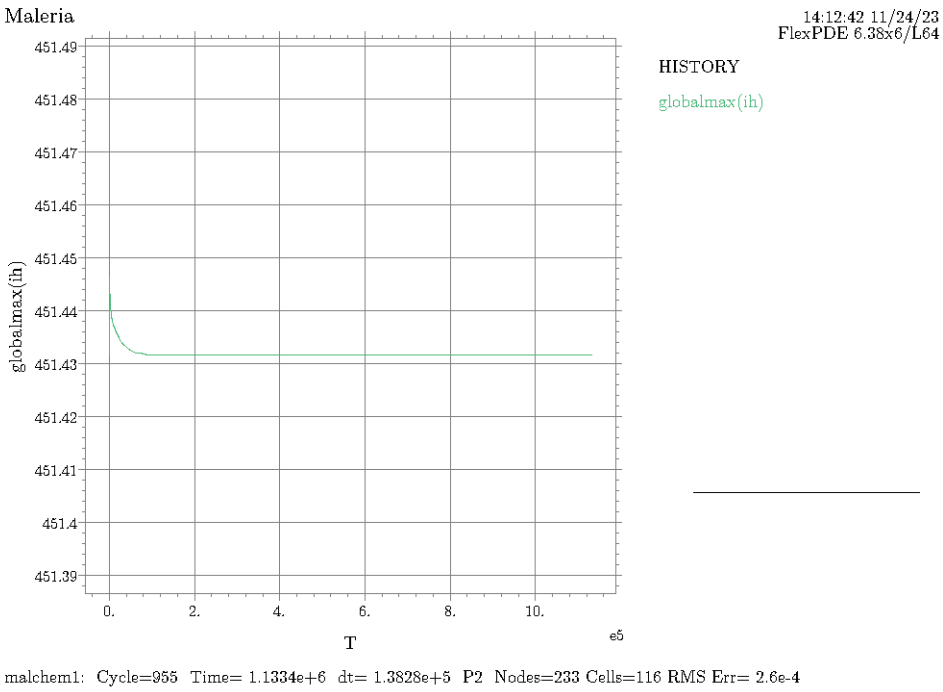

Figure 11: infected humans vs t

Figure 12: Numerical simulation of global maximum from FlexPDE6 of the model (35) showing the of each population in time.

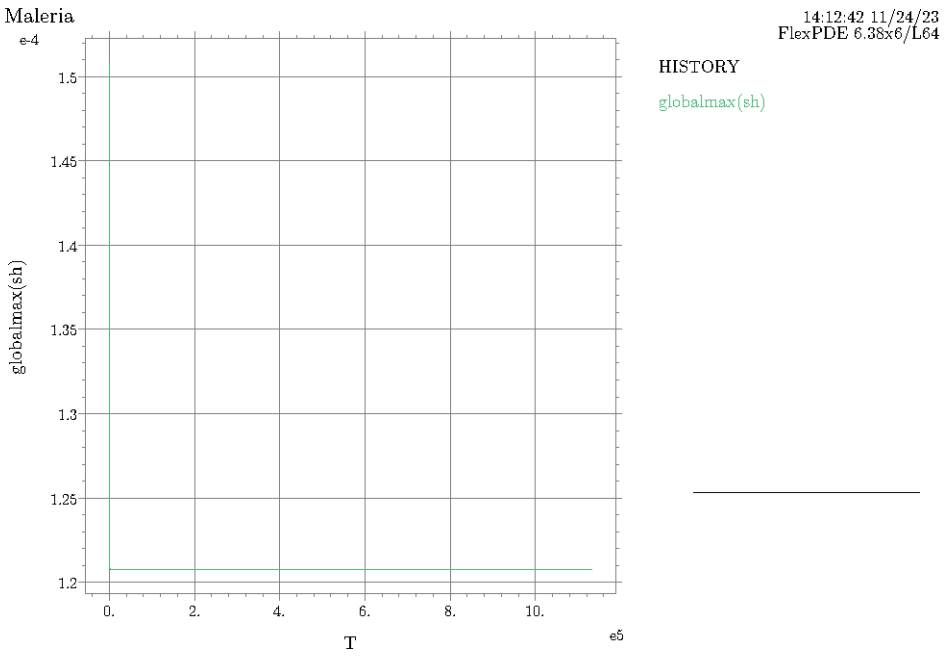

Figure 13: susceptible humans vs t

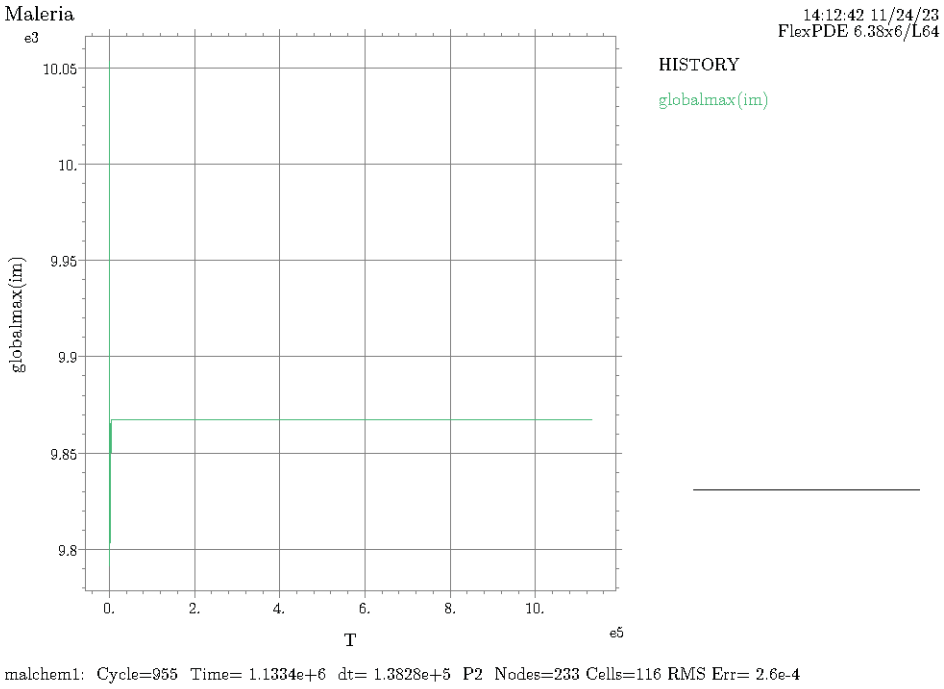

Figure 14: infected mosquitoes vs t

Figure 15: Numerical simulation of global maximum from FlexPDE6 of the model (35) showing the of each population in time.

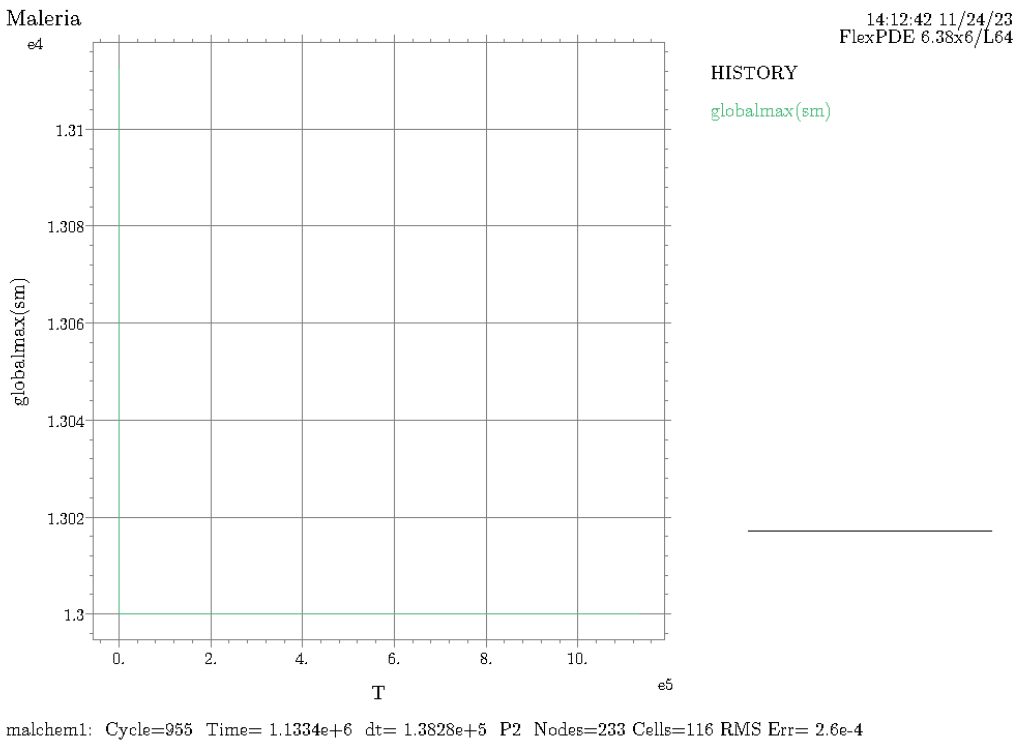

Figure 16: susceptible mosquitoes vs t

Figure 17: Numerical simulation of global maximum from FlexPDE6 of the model (35) showing the of each population in time.

The infected human population initially started at around 451.4435 and reached a global maximum equilibrium of 451.431. The infected mosquito population began at approximately 10.051×10^3 and reached a global maximum equilibrium of about 9.851×10^3. The susceptible human population started at approximately 1.51×10^{-4} and reached a global maximum of around 1.21×10^{-4}. The susceptible mosquito population had an initial value of about 1.315×10^4 and reached a global maximum of 1.3×10^4
Using the above parameter values (44) and these initial conditions, we plotted the solution of model (35) in the domain $(-L, L)$ in FlexPDE6, which resulted in the following;

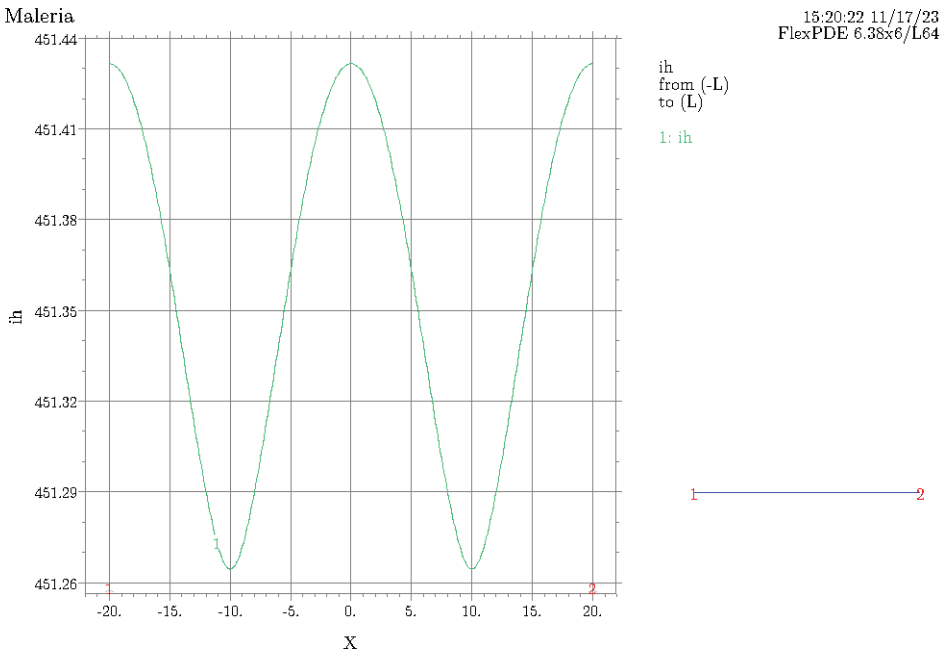

Figure 18: infected humans vs x

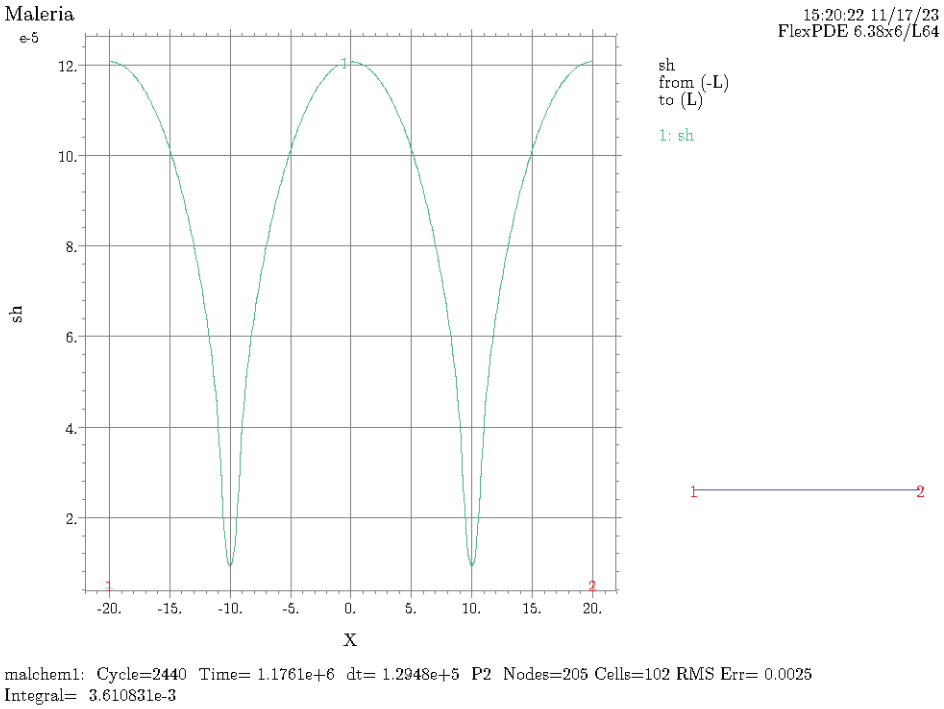

Figure 19: susceptible humans vs x

Figure 20: Numerical simulation in 1D from FlexPDE6 of the model (35) showing the pattern formation of each population in the domain $(-L, L)$.

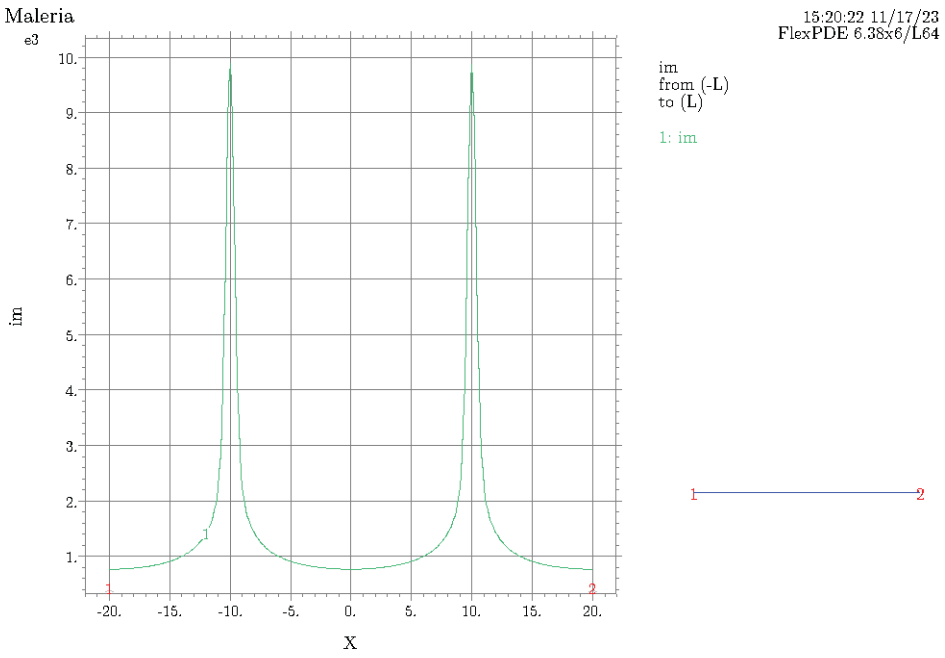

Figure 21: infected mosquitoes vs x

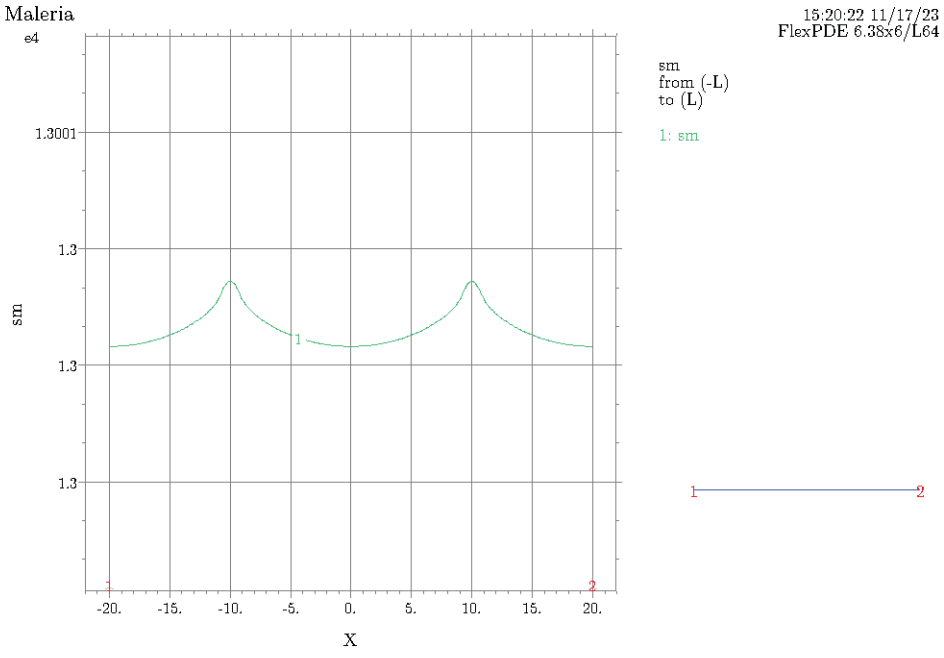

Figure 22: susceptible mosquitoes vs x

Figure 23: Numerical simulation in 1D from FlexPDE6 of the model (35) showing the pattern formation of each population in the domain $(-L, L)$.

The graph presented demonstrates significant spatial changes in the pattern formation of the infected mosquito population (I_m) which results from mosquitoes actively seeking humans and responding to chemoattractants. The graphs for the infected humans population (I_h) and (S_h), show little spatial variation and are nearly constant. The graph for susceptible mosquito population (S_m) shows that they have a lesser impact on human pattern formation compared to infected mosquitoes. Our analysis suggests, that spatially heterogeneous diffusion coefficients and chemotaxis enabled pattern formation on the domain $(-L, L)$ with infected mosquitoes being a major influence just as we predicted.

Chapter 5 Discussion

The primary objective of this research was to investigate the impact of diffusion and chemotaxis on the spatial patterns of malaria transmission in an epidemic model that employs partial differential equations (PDE) and Turing analysis. Undertaken were numerous simulations on Maple, incorporating theoretical concepts derived from alternative models such as the Ross model pertaining to transmission rate parameters, the Keller-Segel model for chemotaxis coefficients, and the renowned Alan Turing's model for diffusion coefficients. For our four-component system, we conducted an eigenvalue analysis, which revealed stable eigenvalues under well-mixed conditions to certain parameter values specified in (44). Our research results suggest that the spatially homogeneous solution $(\bar{I_h}, \bar{S_h}, \bar{I_m}, \bar{S_m})$ is stable in the well-mixed scenario.

We next proceeded to examine our model (35) with only diffusion and no chemotaxis. To determine the allowable frequencies with real positive eigenvalues in the domain $(-L, L)$, we simulated the results of the four eigenvalues and plotted them against frequency (ω). We observed that pattern formation is not possible as none of the eigenvalues exhibit any positive real part. The results leave no room for doubt, indicating the absence of potential pattern formation.

Finally, we analyzed our model (35) using both diffusion and chemotaxis to determine the allowable frequencies with real positive eigenvalues in the interval $(-L, L)$. The graphical representation of these eigenvalues revealed that one eigenvalue has a positive real part within the domain, indicating the potential for pattern formation at specific allowable frequencies between $0 < \omega < 14$. This finding is particularly significant as it suggests that chemotaxis, a key factor in the spread of malaria due to mosquito attraction to humans, plays a crucial role in determining the dynamics of the system.

Following the determination of the parameter values and initial conditions, the model was subsequently numerically simulated using the software FlexPDE6 in the domain extending from $(-L, L)$ in the spatial variable x. The findings of the initial conditions investigation revealed that each population attained the highest level of equilibrium possible and sustained it throughout the simulation. Subsequently, the model given by (35) was graphed in the software package FlexPDE6. The representation depicted the spatial distribution of various populations, specifically those of susceptible humans, infected humans, susceptible mosquitoes, and infected mosquitoes, across the domain spanning from $-L$ to L in the x-domain.

The effect of inclusion of chemotaxis on malaria transmission is that we have highly elevated localized infected mosquito populations which results in more infections in the human population thus leading to a high global human infections. This suggests that chemoattractants in infected humans attracts a greater number of infected mosquitoes, resulting in the formation of patterns. The graph illustrating the infected mosquito population indicates the presence of localized areas in space, which suggests a high concentration of infected humans in those regions. Moreover, the localization of susceptible mosquitoes in the same area as the infected mosquito population suggests that susceptible mosquitoes also have a preference for infected humans over susceptible humans.

Chapter 6 Conclusion

Our study examined the consequences of diffusion and chemotaxis on the spatial distribution of malaria transmission in an epidemic model that utilizes partial differential equations (PDE) to account for both susceptible and infected human and mosquito populations. We employed a Turing analysis to demonstrate that when real eigenvalues are positive and the eigenvalues are stable in well-mixed conditions, a pattern formation can occur in the presence of diffusion and chemotaxis for specific frequencies within a given domain. Furthermore, we presented numerical results that showed distinct patterns for each population and highlighted the impact of diffusion and chemotaxis on maximum initial conditions, which reached equilibrium over time. In conclusion, chemotaxis in infected humans plays a major role in attracting infected mosquitoes and pattern formation.

Our research is constrained in several respects. Firstly, we have no knowledge of the number of individuals who completely recover from malaria, those who receive early treatment, or the duration of susceptibility among partially recovered individuals. We have assumed that partially recovered individuals exhibit lower parasitic levels and therefore lower chemotaxis levels than infected individuals. Future research can be expanded to include factors such as birth rates, latency periods, distance between humans and mosquitoes for both human and mosquito populations, and larger domains. The incorporation of larger domains would result in frequencies converging, and the types of pattern formation and parameter values would also change. Additionally, altering the diffusion coefficients could lead to distinct pattern formations.

Efforts to prevent malaria have been undertaken since the 1950s, but over the years, mosquitoes and parasites have developed resistance to numerous pesticides and drugs. Additionally, the effectiveness of insecticides has diminished as malaria has become resistant to these measures. Among the prevention methods, mosquito nets appear to be the most efficient and durable, without causing disease mutations. However, while these strategies are effective, they do not contribute to our understanding of the transmission of malaria from mosquitoes to humans or among mosquitoes themselves.

One approach to eradicating malaria involves the reintroduction of mosquitoes into affected regions. These mosquitoes are first subjected to genetic modification in laboratory settings and then released into areas where malaria is prevalent. The modified mosquitoes are descendants of those that have developed natural resistance to the disease, which renders them incapable of carrying or transmitting it. As these mosquitoes reproduce in their

natural habitats, their offspring inherit and display similar disease-resistant traits.

References

[1] Roy M Anderson and Robert M May. *Infectious diseases of humans: dynamics and control*. Oxford University Press, 1991.

[2] Joan L Aron. Mathematical modelling of immunity to malaria. *Mathematical Biosciences*, 90(1-2):385–396, 1988.

[3] Jason Bramburger and Matt Holzer. Pattern formation in random networks using graphons. *SIAM Journal on Mathematical Analysis*, 55(3):2150–2185, 2023.

[4] Warren Cornwall. Malaria infection creates a 'human perfume' that makes us more attractive to mosquitoes. 16 April, 2018.

[5] Serkadis Debalke, Tibebu Habtewold, George K Christophides, and Luc Duchateau. Stability of the effect of silencing fibronectin type iii domain-protein 1 (fn3d1) gene on anopheles arabiensis reared under different breeding site conditions. *Parasites & vectors*, 13:1–9, 2020.

[6] João A N Filipe, Eleanor M Riley, Christopher J Drakeley, Colin J Sutherland, and Azra C Ghani. Determination of the processes driving the acquisition of immunity to malaria using a mathematical transmission model. *PLoS computational biology*, 3(12):e255, 2007.

[7] Yandong Gao, Jiashu Sun, Wan-Hsin Lin, Donna J Webb, and Deyu Li. A compact microfluidic gradient generator using passive pumping. *Microfluidics and nanofluidics*, 12:887–895, 2012.

[8] Bryan T Grenfell and Andrew P Dobson. *Ecology of infectious diseases in natural populations*, volume 7. Cambridge University Press, 1995.

[9] Sunetra Gupta and Adrian VS Hill. Dynamic interactions in malaria: host heterogeneity meets parasite polymorphism. *Proceedings of the Royal Society of London. Series B: Biological Sciences*, 261(1362):271–277, 1995.

[10] Sunetra Gupta, Jonathan Swinton, and Roy Malcolm Anderson. Theoretical studies of the effects of heterogeneity in the parasite population on the transmission dynamics of malaria. *Proceedings of the Royal Society of London. Series B: Biological Sciences*, 256(1347):231–238, 1994.

[11] Rafael Gutierrez-Lopez, Josue Martinez-de la Puente, Laura Gangoso, Jiayue Yan, Ramon Soriguer, and Jordi Figuerola. Experimental reduction of host plasmodium infection load affects mosquito survival. *Scientific reports*, 9(1):8782, 2019.

[12] Günther Hasibeder and Christopher Dye. Population dynamics of mosquito-borne disease: persistence in a completely heterogeneous environment. *Theoretical population biology*, 33(1):31–53, 1988.

[13] Thomas Hillen and Kevin J Painter. A user's guide to pde models for chemotaxis. *Journal of mathematical biology*, 58(1-2):183–217, 2009.

[14] Dirk Horstmann. From 1970 until present: the keller-segel model in chemotaxis and its consequences. 2003.

[15] Silvie Huijben and Krijn P Paaijmans. Putting evolution in elimination: winning our ongoing battle with evolving malaria mosquitoes and parasites. *Evolutionary applications*, 11(4):415–430, 2018.

[16] Evelyn F Keller and Lee A Segel. Model for chemotaxis. *Journal of theoretical biology*, 30(2):225–234, 1971.

[17] Lindstrom M. Gumpinger A. C. Zhu J. Coombs D Konrad, B. Assessing the optimal virulence of malaria-targeting mosquito pathogens: a mathematical study of engineered metarhizium anisopliae. *Malaria Journal*, 2014.

[18] Sandip Mandal, Ram Rup Sarkar, and Somdatta Sinha. Mathematical models of malaria-a review. *Malaria journal*, 10(1):1–19, 2011.

[19] Maplesoft, a division of Waterloo Maple Inc.. Maple. `https://hadoop.apache.org`.

[20] Hans Meinhardt. Models of biological pattern formation (academic press, london, 1982). May 1982.

[21] Michael G Neubert, Hal Caswell, and JD Murray. Transient dynamics and pattern formation: reactivity is necessary for turing instabilities. *Mathematical biosciences*, 175(1):1–11, 2002.

[22] Annett Nold. Heterogeneity in disease-transmission modeling. *Mathematical biosciences*, 52(3-4):227–240, 1980.

[23] World Health Organization. World malaria report 2022. 8 December 2022.

[24] Diego J Rodríguez and Lourdes Torres-Sorando. Models of infectious diseases in spatially heterogeneous environments. *Bulletin of Mathematical Biology*, 63(3):547–571, 2001.

[25] Ronald Ross. Some a priori pathometric equations. *British medical journal*, 1(2830):546, 1915.

[26] Lisa Sattenspiel and Klaus Dietz. A structured epidemic model incorporating geographic mobility among regions. *Mathematical biosciences*, 128(1-2):71–91, 1995.

[27] Lisa Sattenspiel and Carl P Simon. The spread and persistence of infectious diseases in structured populations. *Mathematical Biosciences*, 90(1-2):341–366, 1988.

[28] Maria Vladimirovna Shubina. Exact traveling wave solutions of one-dimensional parabolic–parabolic models of chemotaxis. *Russian Journal of Mathematical Physics*, 25:383–395, 2018.

[29] OT Soniran, OA Idowu, OL Ajayi, and IC Olubi. Comparative study on the effects of chloroquine and artesunate on histopathological damages caused by plasmodium berghei in four vital organs of infected albino mice. *Malaria Research and Treatment*, 2012, 2012.

[30] Lourdes Torres-Sorando and Diego J Rodrıguez. Models of spatio-temporal dynamics in malaria. *Ecological modelling*, 104(2-3):231–240, 1997.

[31] Imelda Trejo, Martha Barnard, Julie A Spencer, Jeffrey Keithley, Kaitlyn M Martinez, Isabel Crooker, Nicolas Hengartner, Ethan O Romero-Severson, and Carrie Manore. Changing temperature profiles and the risk of dengue outbreaks. *PLOS Climate*, 2(2):e0000115, 2023.

[32] Alan Mathison Turing. The chemical basis of morphogenesis. *Bulletin of mathematical biology*, 52:153–197, 1990.

[33] Yang O Zhao, Sebastian Kurscheid, Yue Zhang, Lei Liu, Lili Zhang, Kelsey Loeliger, and Erol Fikrig. Enhanced survival of plasmodium-infected mosquitoes during starvation. *PLoS One*, 7(7):e40556, 2012.

Appedices

A FlexPDE6 Code

```
TITLE 'Maleria'

COORDINATES cartesian1
VARIABLES
 ih
 sh
 im
 sm

SELECT         { method controls }

errlim=1.5e-3

DEFINITIONS
Dh1=1 {Infected diffusivity}
Dh2=1 {Susceptible diffusivity}
Dm=.25
C=150
{C=0}
mu=.00025{Mosquito infection}
nu=.002 {Recovery Rate}
beta=10


r=20 {mosquito reproduction rate}
N=13000 {Mosquito Population}
Nh=100
r2=2
imdr=1
ihdr=.00004
```

```
L=20

transfer('mal.ic',ih0,sh0,im0,sm0)

 INITIAL VALUES
sh=1000+.2*cos(.2*x)*0

ih=1+.01*cos(.2*x)*0
im=100+.2*cos(.2*x)
sm=100+.2*cos(.2*x)

sh=sh0
ih=ih0
im=im0
sm=sm0

EQUATIONS
ih: dt(ih)=Dh1*dxx(ih)+beta*sh*im-nu*ih-ihdr*ih
sh: dt(sh)=Dh2*dxx(sh)-beta*sh*im+nu*ih+r2*sh*(Nh-sh)

im: dt(im)=Dm*dxx(im)+mu*ih*sm-imdr*im+C*dx(im*dx(ih))+C/10*dx(im*dx(sh))
sm: dt(sm)=Dm*dxx(sm)+r*(sm)*(N-(sm))-mu*ih*sm+C*dx(sm*dx(ih))+C/10*dx(sm*dx(sh))



BOUNDARIES

  REGION 1       { For each material region }
    START(-L)
    point natural(ih)=0 point natural(sh)=0  point natural(im)=0  line to (L) point natu
TIME 0 TO 1500000
MONITORS
!for t=0 by 1 to 200
for cycle = 5

  elevation(ih) from (-L) to (L)
```

```
  elevation(sh) from (-L) to (L)
 elevation(im) from (-L) to (L)
 elevation(sm) from (-L) to (L)

plots
for cycle=5
transfer(ih,sh,im,sm) file "y.dat"
history(globalmax(ih))
history(globalmax(sh))
history(globalmax(im))
history(globalmax(sm))
end
```

B FlexPDE6 Code 2D

```
TITLE 'Maleria'

COORDINATES cartesian2
VARIABLES
 ih
 sh
 im



SELECT         { method controls }
errlim=5e-1
DEFINITIONS
Dh1=1
Dh2=1
CT=.1
Dm=.01
beta=2
mu=.01
nu=.5
```

```
N=1000
delta=1

L=50

 INITIAL VALUES
sh=100+20*cos(5*x*y)
ih=1+.1+cos(5*x*y)
im=10+.2*cos(5*x*y)


EQUATIONS
ih: dt(ih)=Dh1*div(grad(ih))+beta*sh*im-nu*ih
sh: dt(sh)=Dh2*div(grad(sh))-beta*sh*im+nu*ih

im: dt(im)=Dm*div(grad(im))+mu*ih*(N-im)+div(CT*(im*grad(ih+sh)))

BOUNDARIES
  REGION 1

START(L,0)

ARC(CENTER=0,0) ANGLE=360
```